IOPscience iopscience.iop.org

Home Search Collections Journals About Contact us My IOPscience

Boron in tungsten: electronic structure and ordering tendencies

This article has been downloaded from IOPscience. Please scroll down to see the full text article.

2000 J. Phys.: Condens. Matter 12 4175

(http://iopscience.iop.org/0953-8984/12/18/303)

View the table of contents for this issue, or go to the journal homepage for more

Download details:
IP Address: 171.66.16.221
The article was downloaded on 16/05/2010 at 04:52

Please note that terms and conditions apply.

J. Phys.: Condens. Matter **12** (2000) 4175–4186. Printed in the UK PII: S0953-8984(00)10181-X

Boron in tungsten: electronic structure and ordering tendencies

Simon Dorfman

Department of Physics, Israel Institute of Technology—Technion, 32000 Haifa, Israel

Received 8 December 1999, in final form 24 February 2000

Abstract. In the framework of linear density functional theory, the conditions of formation of tungsten–boron interstitial solid solutions are studied. On the basis of the coherent-potential approximation, the ordering tendencies in tungsten-based solid solutions are considered and the possibility of formation of some type of ordering on the sublattice of the interstitial octahedral positions is demonstrated. The tendencies of the chemical bonding in the interstitial solid solution of boron in tungsten are discussed.

(Some figures in this article are in colour only in the electronic version; see `www.iop.org`)

1. Introduction

The large cohesive energy and bulk modulus of tungsten and molybdenum have led to wide use of these refractory metals in industry and have been the topics of a lot of investigations in materials science. Measuring of high-pressure properties of W and Mo is a serious problem because of their extremely low compressibility. That is why any predictions of the behaviour of these metals in extreme conditions are of value. Non-empirical calculations for tungsten were used to study the influence of microalloying on the ductile–brittle phase transformation [1]. In tungsten, impurities such as N, O, P, S, and Si weaken the intergranular cohesion, resulting in 'loosening' of the grain boundary (GB). The presence of B and C, in contrast, enhances the interatomic interaction across the GB.

In the case of many metals and alloys, small boron additions modify their ambient temperature properties (see, for example, reference [2]). Some intermetallic alloys which present an intrinsic intergranular brittleness in their undoped state change their fracture mode when boron doped. In some cases—like in the B-doped hypostoichiometric Ni_3Al alloys—the fracture becomes ductile. In other cases, like in FeAl (B2) alloys, even in the B-doped alloys a brittle fracture is observed, but it takes place in a transgranular manner, by cleavage [3, 4].

The boron effects in metals and alloys are typically attributed to its intergranular segregation. This hypothesis is based on experimental measurements of some intergranular boron enrichment, mainly in Ni_3Al alloys, by Auger electron spectroscopy (AES) [5]. Tungsten-based solid solutions were simulated non-empirically [1, 6]; as a result, the idea was formulated that the cohesion of the GB may be the controlling factor which limits the ductility of high-strength metallic alloys, and particularly those containing W. B in the GB has the lowest energy and thus would tend to displace other impurity atoms from the GB. Microalloying with 10–50 ppm B may be an effective way of improving tungsten's ductility. These results are important for understanding the fundamental physics of intergranular embrittlement. As a result, a number of papers were devoted to the modelling of tungsten GBs in different

0953-8984/00/184175+12$30.00 © 2000 IOP Publishing Ltd

approaches (see, for example, [7] and references therein). However, as far as we know no systematic study of the tungsten-based solid solution as regards its ordering and bonding tendencies and thermodynamic aspects is available in the literature.

In the framework of linear density functional (LDF) theory, the conditions of formation of W–B solid solutions for different concentrations of boron are studied. On the basis of the coherent-potential approximation (CPA) we consider the ordering tendencies, study the electronic structure and provide total-energy calculations.

2. The LDA model

The essential requirement for such research is to have a reliable and efficient electronic structure method for calculation of the total energies and electronic structures of the interstitial solid solutions of tungsten. Within the framework of the Hohenberg–Kohn–Sham density functional theory (DFT) the electronic structure can be efficiently handled using first-principles self-consistent methods. DFT has wide applications to molecules and solids [8]. Even the crudest approximation, local density approximation (LDA), to the density functional theory has been successfully applied to predict structural and dynamical properties of a large variety of materials. Equilibrium volumes, elastic constants, phonon frequencies, surface reconstruction, and magnetism are just some examples of properties which could be successfully calculated for systems without particularly strong electron correlations within the LDA. The LDA usually leads to some overbinding in solids (equilibrium volumes are typically 1–3% underestimated). Considerably larger errors are found in cases where the LDA is not sufficiently accurate; ionic compounds like MgO are examples where the simple LDA fails.

The electronic structure of crystalline solids could be efficiently calculated using linear band-structure methods. The linear muffin-tin orbitals (LMTO) method is particularly fast and efficient for handling complex and large unit cells because of the ease with which the structure-dependent part and the potential-dependent part are separated out in the secular equation [9]. An important milestone in the application of the LMTO method was understanding that the original infinite LMTO basis set can be limited to just a few orbital functions. With this advantage, the LMTO method has the computational simplicity of the empirical tight-binding schemes, as well as the accuracy of other first-principles methods.

The LMTO method in the atomic sphere approximation (ASA) approach is a well-established technique for studying metals, alloys, and also perovskites and different phases with non-trivial structures [10–13]. For close-packed metallic structures, in particular, this method consistently predicts reliable and accurate results comparable to those obtained from other sophisticated LDA-based methods like the linearized augmented-plane-wave (LAPW) technique [14]. In the last few years, the LMTO ASA method has been successfully applied also to the study of surface alloys (see, for example, [15]). In the case of dilute alloys, the properties of Fe embedded in V and Cr matrices were studied in [15]. It seems that today this scheme is one of the most promising techniques in band-structure studies due to its ability to calculate very complicated structures very fast. The LMTO ASA method is ideally suited to the relatively close-packed solid solutions of tungsten treated here, where one can ensure a reasonably small overlap between the atomic spheres. We controlled the value of this overlap by introducing an additional interstitial ('empty') sphere. In the LMTO ASA, the approximation due to spherical averaging can also be controlled by changing the ratio between atomic spheres of different species. The overlap between the spheres is defined as $(S_1 + S_2 - d) \times 100/(2S_1)$ and is less than 30%. Here S_1 and S_2 ($S_1 < S_2$) are the radii of the two overlapping spheres and d is the distance between them. Incorporating the so-called 'combined corrections', one can partly correct the error due to spheridization of the potential and charge density [9].

Band-structure calculations based on the density functional theory allow one to obtain a quantitative description of the ground-state properties of absolutely ordered alloys. Application of these methods to the calculations of the thermodynamic properties of partially ordered or random alloys gives reasonable results [16–20]. The most attractive feature of the single-site (SS) coherent-potential approximation (CPA) is that this scheme can be applied to direct calculations of the electronic structure of randomly or partially ordered alloys [17]. Recent applications of the CPA scheme show that this method allows one to reproduce accurately lattice parameters, bulk moduli, and enthalpies of formation (see, for example, reference [18] and references therein). This accuracy is similar to the accuracy of other local density functional methods for completely ordered phases.

In order to study the effects of the electronic density distributions in tungsten-based solid solutions on the chemical bonding, we model interstitial solid solutions with a cell shown in figure 1. The behaviour of the boron atoms in the tungsten is studied on the basis of first-principles total-energy calculations of binary, partially ordered compounds in the framework of the CPA.

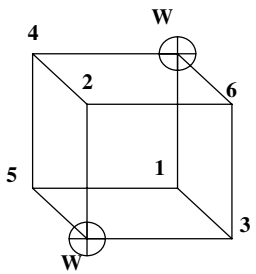

Figure 1. The structure of the cell used in the CPA LMTO simulations. The numbers indicate the sublattices of octahedral interstitial positions: on the first sublattice they are numbered 1 and 2, on the second sublattice they are numbered 3 and 4, and on the third sublattice they are numbered 5 and 6. The crossed circles show tungsten atoms.

We present here only a brief outline of the technique of the usual SS CPA for solids with several different sublattices [18]. Let us consider an interstitial bcc solid solution W_cB_{1-c}, where B occupies the octahedral interstitial sites of the bcc lattice and c is the atomic fraction of W. There are three equivalent bcc sublattices of such interstitial sites. If in each of these sublattices, enumerated by p ($p = 1, 2, 3$), N_p sites of the total of N sites of a sublattice are occupied by boron atoms, then $c_p = N_p/N$ is the atomic fraction of boron on the corresponding sublattice and

$$c = N \Big/ \left(N + \sum_{p=1}^{3} N_p \right) = 1 \Big/ \left(1 + \sum_{p=1}^{3} c_p \right). \tag{1}$$

.

To study the ordering in the interstitial solid solution, it is convenient to determine the probability $n_p(\vec{r})$ of finding an interstitial atom in the position $\vec{r}$ on the pth sublattice. This ordering is considered as the ordering between interstitial atoms and 'empty' sites in each sublattice. It is worth mentioning that actually two types of ordering may occur in the case where there are several equivalent sublattices of interstitial sites. One type of ordering corresponds to the situation where, for example, interstitial atoms occupy only one (say, $p = 1$) sublattice of interstitial positions, leaving all the rest of the sublattices empty ($n_2 = n_3 = 0$). In this case the interstitial atoms may still be randomly distributed on the sites of this sublattice. Decrease of the temperature may result in ordering on this sublattice, and in this situation

$n_{p=1}(\vec{r})$ takes several constant values. Each value defines a sub-sublattice of the ordered phase, which is formed on the first sublattice of interstitial sites. If, in the simplest case, the B2-type ordered phase is formed on the first sublattice of interstitial sites, then for a stoichiometric composition ($c_1 = 1/2$):

$$n_1^{(1)} = c_1 + \frac{1}{2}\eta = 1$$

for the corners of the bcc cubic cell of the first interstitial sublattice; and

$$n_1^{(2)} = c_1 - \frac{1}{2}\eta = 0$$

for the centres of the same cell. In these expressions, the upper index enumerates sublattices, and η is the long-range order parameter, which is defined on the first sublattice in the usual manner: $\eta = (n_1^{(1)} - c_1)/(1 - c_1)$ (see, for example, [21]). The probabilities of finding empty sites are defined as $(1 - n_p)$, and the corresponding equations for them may also be written down.

Now we are ready to redefine the probabilities $n_p(\vec{r})$ in the vector form. The components of this vector determine the occupation of the octahedral sublattices by interstitial atoms. The vector which corresponds to the formation of a B2-type phase on the first sublattice, with empty second and third sublattices, is given by $\vec{n} = \{n^{(i)}\}\big|_{i=1,\ldots,6}$ as follows:

$$\vec{n} = \left(c_1 + \frac{1}{2}\eta, c_1 - \frac{1}{2}\eta, 0, 0, 0, 0\right). \tag{2}$$

For example, for the specific case ($c_2 = c_3 = 0$) with the atomic fraction of boron equal to 0.01 and the atomic fraction of tungsten equal to 0.99, the corresponding value c_1 may be found from the equation

$$0.99 = \frac{1}{1 + c_1}$$

which gives $c_1 = 0.010\,101$, and for the atomic fraction of B equal to 0.167 it gives the value $c_1 = 0.200\,48$.

The average one-electron Green's function should be determined for calculations of electronic structure and ground-state properties. To obtain this function, we apply the SS CPA in conjunction with the LMTO method in the atomic sphere approximation (ASA). The average one-electron Green's function may be obtained in the form of the Korringa–Kohn–Rostoker (KKR) ASA Green's function, which is identical to the scattering path operator in multiple-scattering theory. For a complex energy z, we have

$$\Gamma_{ij}(z) = \frac{1}{V_{BZ}} \int_{BZ} \mathrm{d}^3k \, [\Re(z) - \Lambda(\boldsymbol{k})]^{-1}_{ij} \tag{3}$$

where V_{BZ} is the volume of Brillouin zone (BZ), $\Lambda(\boldsymbol{k})$ are the LMTO structure constants, and $\Re(z)$ is the crystal coherent-potential matrix. The subscripts i and j refer to individual sub-sublattice sites in the unit cell. We have omitted the angular momentum quantum numbers (l_m) as well as the LMTO representation number. The coherent-potential matrix that enters equation (3) is block diagonal:

$$\Re = \begin{pmatrix} \Re_1 & 0 & \cdots & 0 \\ 0 & \Re_2 & \cdots & 0 \\ \cdots & \cdots & \cdots & \cdots \\ 0 & 0 & \cdots & \Re_n \end{pmatrix} \tag{4}$$

and each diagonal element $\Re_i$ is the coherent-potential function of the sub-sublattice i. To obtain the complete coherent-potential function, we must solve for each sub-sublattice corresponding equations, which for our case are

$$\begin{aligned} \Re_i &= n^{(i)}\Re_i^{\mathrm{B}} + (1-n^{(i)})\Re_i^{\mathrm{E}} + [\Re_i^{\mathrm{B}} - \Re_i^{\mathrm{E}}]\Gamma_{ii}[\Re_i^{\mathrm{B}} - \Re_i^{\mathrm{E}}]\big|_{i=\{1,2\}} \\ \Re_i &= \Re_i^{\mathrm{E}} + \Re_i^{\mathrm{E}}\Gamma_{ii}\Re_i^{\mathrm{E}}\big|_{i=\{3,\ldots,6\}} \end{aligned} \tag{5}$$

where $n^{(i)}$ is the occupation probability for boron-atom sites on the ith sub-sublattice, and $\Re_i^{\mathrm{B}}$ and $\Re_i^{\mathrm{E}}$ are the coherent-potential functions of the B and E species, respectively. 'E' here stands for an empty interstitial site, or 'empty' sphere in the ASA. Coherent-potential functions are coupled by the definition (equation (3)) of the coherent Green's function, which, together with equation (5), forms the non-linear system of CPA equations that must be solved self-consistently.

We calculated the electronic density distributions with the CPA LMTO code [11, 18]. This code includes the determination of the Madelung-energy prefactor ζ, which makes the CPA LMTO results agree with those obtained by the Connolly–Williams method on the basis of the total energies of ordered alloys [16]. This prefactor enters the expression for the Madelung energy of the alloy and, for the ith sub-sublattice of the tungsten-based interstitial solid solution, this is

$$E_{Mad}^{(i)} = -\zeta e^2 n_{\mathrm{B}}^{(i)}(1-n_{\mathrm{B}}^{(i)})\frac{(Q_{\mathrm{B}}-Q_{\mathrm{E}})^2}{R^{(i)}(1)}. \tag{6}$$

Here $R^{(i)}(1)$ is the radius of the first coordination shell of the ith sub-sublattice, e is the electron charge, and the boron and empty-sphere charges are Q_{B} and Q_{E}, respectively. These charges are defined as

$$Q_{\mathrm{B}} = \int_{S_{ASA}} \rho_{\mathrm{B}}\,\mathrm{d}^3r - Z_{\mathrm{B}} \qquad Q_{\mathrm{E}} = \int_{S_{ASA}} \rho_{\mathrm{E}}\,\mathrm{d}^3r.$$

In these equations S_{ASA} is the radius of an atomic sphere, Z_{B} is the atomic number of boron, and ρ_{B} and ρ_{E} are the electronic densities of a boron atom and an empty sphere, respectively. A number of models could be reduced to these equations [19].

3. Calculations

Our study is based on the analysis of electronic density distributions for different interatomic distances, supercell configurations, and compositions of an interstitial impurity. Changes in the concentration will lead to changes of the supercell volume and to changes in the character of the bonding forces. Band structures of completely ordered tungsten-based interstitial alloy with partially occupied octahedral positions 1 and 2 (see figure 1):

$$\text{site 1} \rightarrow \left(\frac{1}{2}\frac{1}{2}0\right) \qquad \text{site 2} \rightarrow \left(00\frac{1}{2}\right)$$

were carried out within the CPA LMTO procedure briefly outlined in the previous section (for details see references [15] and [18]). With the self-consistently obtained bands, we calculated the equilibrium total energies of the completely ordered phase and phases with partially occupied sublattices.

In our calculations we studied the behaviour of the dilute solid solutions of boron in tungsten. According to Hagg's rule, we assumed that these solutions are interstitial, because the ratio of the atomic radii of the constituents is less than 0.49. Boron atoms were distributed on one of three sublattices of octahedral interstitial positions of the host matrix. Such a modelling had two main aims: (a) to study the tendencies of ordering of boron atoms on one

of interstitial sites sublattices in tungsten; and (b) to obtain information about the bonding tendencies for boron atoms in tungsten media.

The calculations were performed in the scalar-relativistic approach for a number of different volumes per atom. Core electrons were frozen after initial atomic calculations. All of the calculations were done in the framework of the atomic sphere approximation (ASA) [9]. The individual atomic sphere radii of W, B, and empty (E) spheres were set in the ratio 1:0.6:0.6 respectively. The convergence criterion for the total energy was 0.001 mRyd. Typically 60 iterations were needed to achieve the necessary convergence. The equilibrium lattice parameter and corresponding ground-state energy of a given alloy were obtained on the basis of a set of self-consistent calculations of the total energy close to the equilibrium lattice parameter with a fit to a Morse-type equation of state [22]. In figure 2 we show plots of the total density of states (DOS) for W–B interstitial solid solutions with different concentrations of B placed in position 1 of the first sublattice (see figure 1). DOSs correspond to different compositions of interstitial W–B solid solutions with the equilibrium lattice parameter. The integration over the Brillouin zone was performed with the special-points technique (the number of points was about 250).

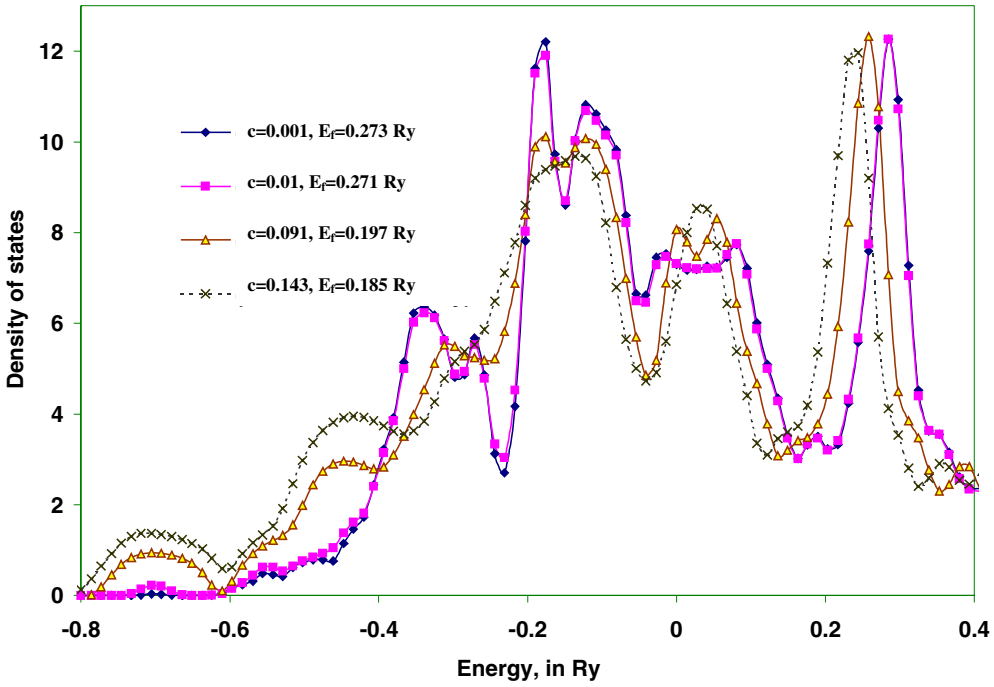

Figure 2. The total density of states (in number of states per atom per Ryd) in interstitial W–B solid solutions for different atomic fractions of boron. E_f in the figure is the Fermi energy. c is the boron occupation of position 1 (see figure 1). A solid solution is studied for the ordered state with the partial occupation of only one sublattice.

At the first step of the calculations, we investigated the structure where boron occupies, with small concentrations, only the corners of one cubic primitive cell of octahedral interstitial positions. At each stage of the calculations, i.e. at all of the concentrations studied, the lattice parameter was varied to obtain the minimal total energy. The increase of boron concentration has an opposite effect on the partial total energies: the tungsten energy decreases while the

boron energy increases. The same opposite tendency is illustrated by table 1: the total number of states at the Fermi energy for W increases while for B it decreases with the growth of the boron concentration. At the same time the total energy per atom for dilute W–B interstitial solid solutions decreases, as well as the Fermi energy. The partial numbers of s and p states for W show a stable tendency to increase with the rising boron concentration while the numbers of s and p states for B decrease. This is not the case for the behaviour of the number of d states. For W it increases, while for boron it decreases as concentration grows, and at concentration $c_B = 0.167$ starts to increase, showing thus a non-monotonic behaviour. In figure 3 we present the dependence of the energy per atom on the lattice parameter for two concentrations of extremely dilute solid solutions. The curves presented show non-trivial behaviour. We may analyse these curves in terms of enthalpy because the pressure–volume term, in the units which are used for the calculations, is negligibly small. The 'caving' in the curve between points 1 and 2 in this figure shows that for the lattice parameter 6.2 au and for the atomic fraction of boron equal to 0.001, the tungsten-based solid solution is unstable. Thus the two-phase mixture of dilute solid solutions with lattice parameters 6.14 au and 6.26 au is preferable to the one-phase state of the solid solution. This means that although for pressure equal to zero the one-phase state with the lattice parameter $a = 6.14$ au is stable, when tensile stress is

Table 1. Total number of states, T_{NS} (in number of states per atom per Ryd), for tungsten and boron atoms at the Fermi energy, E_F, and total energy, E_{tot}, per cell for W–B dilute solid solutions.

Atomic fraction of B, c_B	Number of states, T_{NS}, for W	Number of states, T_{NS}, for B	Fermi energy, E_F, in Ryd	Total energy, E_{tot}, in Ryd
0.0005	4.959	2.555	0.273	−32.224
0.005	4.975	2.550	0.272	−32.320
0.048	5.186	2.518	0.197	−33.384

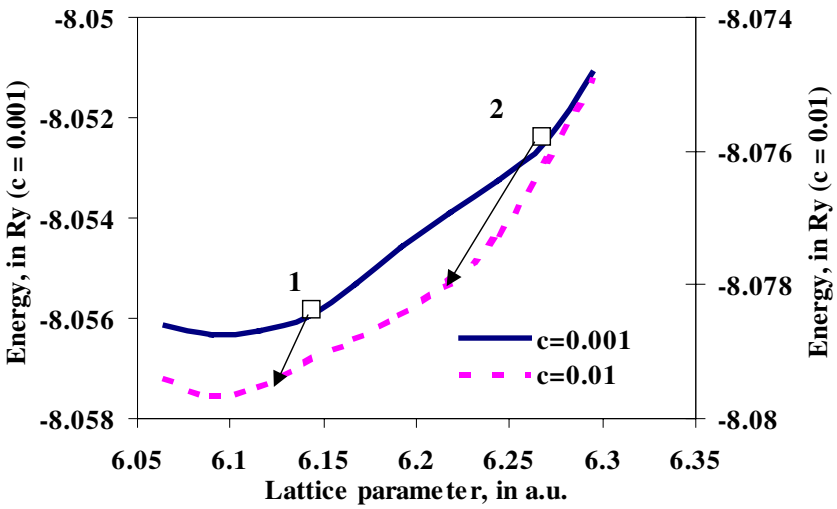

Figure 3. Dependencies of the total energy per atom for interstitial W–B solid solutions on the lattice parameter for different atomic fractions of boron. A solid solution is studied for the ordered state with the partial occupation of only one sublattice. The left Y-axis gives energies for $c = 0.001$ and the right one gives energies for $c = 0.01$. c_B is the boron occupation of position 1 (see figure 1). Boxes 1 and 2 show the region with the positive curvature in the energy plot for $c = 0.001$. Arrows show the direction of the shifts of this curvature with concentration change.

applied the solid solution decomposes into a two-phase state. When the concentration of boron increases, the effect weakens, as shown by the dashed line in figure 3, and it vanishes at larger concentration of boron. Decrease of the B concentration will shift the higher local minimum of the total-energy curve in figure 3 to infinity, decreasing the 'caving' of the curve. In this case, the instability will certainly disappear for lower B concentration. From figure 4 it follows that the equilibrium lattice parameter of the interstitial solid solution of boron in tungsten is a non-linear function of the atomic fraction of boron. It may be seen in figure 4 that for extremely small boron concentration the lattice parameter has an anomalous behaviour. The analysis of this figure shows that the coefficient of concentration dilatation of the lattice is negative for all atomic fractions of B until the boron concentration equals 0.006; it becomes equal to zero for this composition, and after this it becomes positive and concentration independent.

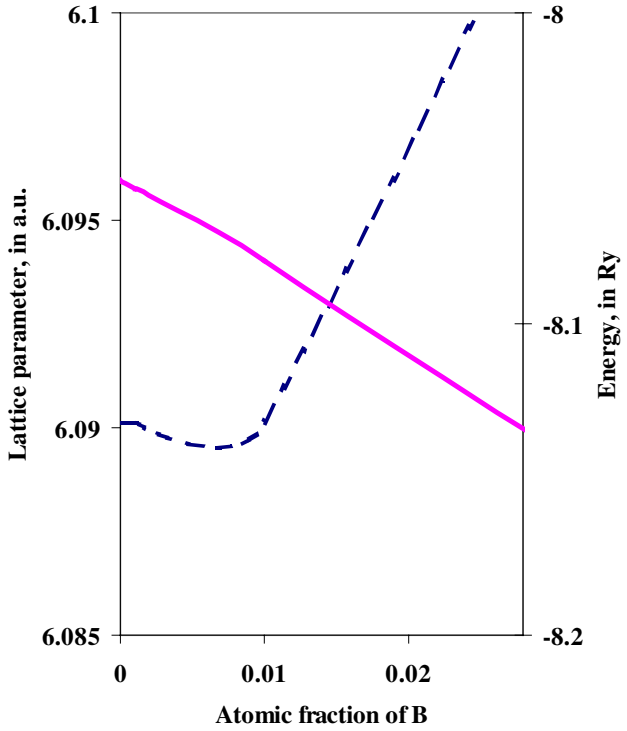

Figure 4. Dependencies of the lattice parameter (dashed line) and the energy (solid line) of tungsten–boron alloy on the boron occupation of position 1 in figure 1. A solid solution is studied for the ordered state with the partial occupation of only one sublattice.

One of the goals of our investigation was to study ordering tendencies in W–B solid solutions. To this end, we studied the different possibilities of occupations of the sites of one or two sublattices of the octahedral positions of boron atoms. The results of this study are given in tables 2 and 3. In table 2 total energies of different occupations of sublattices are compared for the same atomic fraction of B. This result demonstrates the tendency for boron atoms to occupy only one of the octahedral interstitial sublattices. In table 3 we show how the occupation ratio influences the equilibrium Wigner–Seitz radius and the total energy of the solid solution for boron occupying only one sublattice. This occupation ratio at a given atomic fraction of B atoms in a W_cB_{1-c} interstitial alloy shows how B atoms are distributed between sub-sublattices 1 and 2, while sub-sublattices 3, . . . , 6 remain empty. In this way, we model the

Table 2. Total energies, E_{tot}, per cell for W–B solid solution for different boron occupations of the sites $1|_{(1/2,1/2,0)}$, $2|_{(0,0,1/2)}$, $3|_{(0,1/2,0)}$, and $4|_{(1/2,0,1/2)}$ in the first and the second sublattices of octahedral interstitial positions.

	Occupation ratio				
	First sublattice		Second sublattice		
Boron occupation of interstitial positions	1	2	3	4	E_{tot} in Ryd
0.2	0.5	0.5	0.5	0.5	−34.3273
0.2	1	0	0	0	−34.3463

Table 3. Total energies, E_{tot}, per cell for W–B solid solutions, and the equilibrium Wigner–Seitz radius, R_{WS}, for different boron occupations of the sites $1|_{(1/2,1/2,0)}$ and $2|_{(0,0,1/2)}$ in the first sublattice of octahedral interstitial positions. In the last three lines, $c_B = 0.33$.

	Occupation ratio		
R_{WS} in au	Position 1	Position 2	E_{tot} in Ryd
2.38	0	0	−32.216
2.45	1	0	−37.656
2.44	0.9	0.1	−37.576
2.44	0.5	0.5	−37.436

ordering of boron on one sublattice of octahedral interstitial positions. Thus, for example, the occupation ratio 1:0 means that all B atoms occupy sub-sublattice 1. This situation corresponds to maximal order of B2 type for the corresponding atomic fraction of B. The occupation ratio 0.5:0.5 corresponds to the random distribution of B between sub-sublattices 1 and 2. This is the absolutely disordered interstitial solid solution on the sublattice, defined by n_1. At the same time this state of the alloy may be still considered as an ordered one in the sense that two other octahedral interstitial site sublattices are absolutely empty ($n_2 = n_3 = 0$).

The results presented clearly demonstrate the tendency to form a B2 phase (CsCl-type) on the sublattice of octahedral interstitial positions. This B2 phase consists of boron atoms, which occupy the corners of the cubic cell of the sublattice, while the centres of this cell are empty. Such a configuration is seen to be favourable in comparison with others if energies are compared. The plots of density of states displayed for different concentrations of boron (figure 2) show an increased concentration of bands in the low-energy region (between −0.6 and −0.8 Ryd) with increase of the boron concentration in the alloy. This fact indicates the formation of chemical bonding in W–B solid solutions. Analysis of the partial contributions to this band shows that the band is formed mainly by s and p orbitals of tungsten and s orbitals of boron (see figures 5(a) and 5(b)). The DOS at the Fermi level, $N(E_F)$, is an important quantity, as it is used for the estimation of the electronic specific heat and the electron–phonon coupling constant, and even for determining the vibration contribution to the entropy at finite temperature. The value of $N(E_F)$ reflects the trend towards metallicity in these solid solutions. Figure 6 displays the behaviour of the total density of states in the vicinity of the Fermi energy. It is seen that increase of the atomic fraction of boron leads to decrease of the number of states at the Fermi level, thus decreasing the degree of metallicity in the system. At the same time, for $c_B = 0.2$ we find once more an increase of $N(E_F)$. This conclusion is confirmed by the results given in table 3, which shows the non-monotonic change of the number of states at the Fermi energy, $N(E_F)$, as a function of the boron concentration.

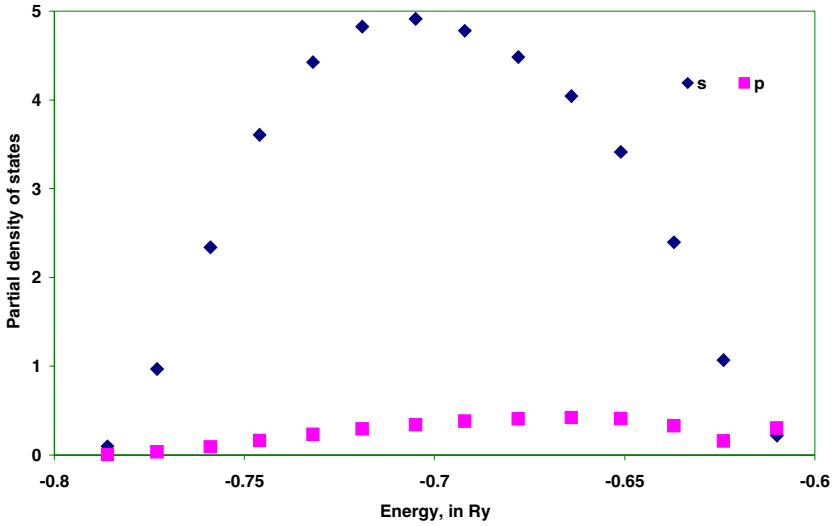

(a)

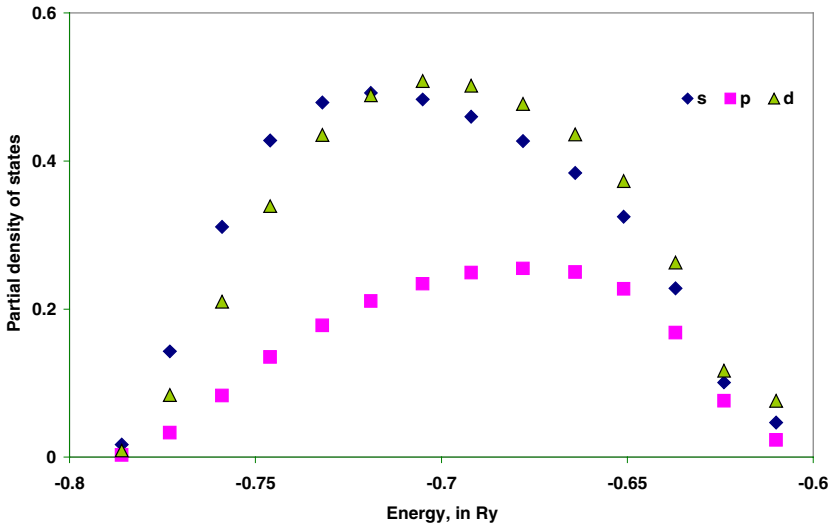

(b)

Figure 5. Partial density of states (PDOS—in numbers of s, p, d states per atom per Ryd) for the boron occupation of position 1 in figure 1 equal to 1%. (a) Plots for boron; (b) plots for tungsten. An interstitial solid solution is studied for the ordered state with the partial occupation of only one sublattice.

4. Summary

In this paper we studied the electronic structure and the total-energy characteristics of extremely dilute interstitial tungsten–boron solid solutions. We discussed the tendencies of the chemical bonding in such solutions and showed that ordering on the sublattice of interstitial octahedral positions could occur. We presented the results of non-empirical calculations, which predict anomalous behaviour of the coefficient of concentration dilatation of the lattice and formation

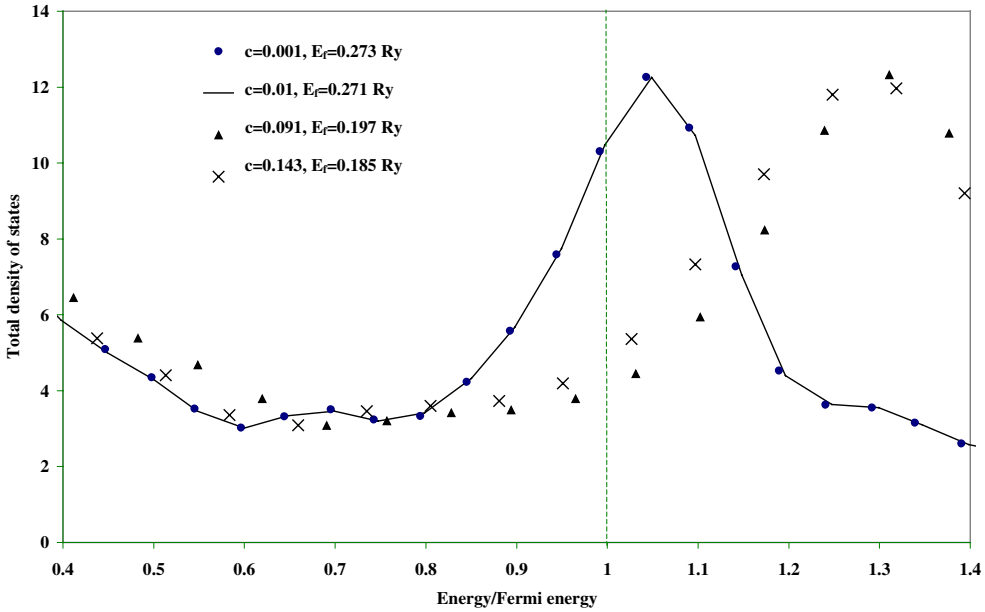

Figure 6. Dependencies of the total density of states (in number of states per atom per Ryd) on the energies normalized to the Fermi energy, E_f in the figure, in interstitial W–B solid solutions for different atomic fractions of boron in the Fermi energy region. c is the atomic occupation of position 1 in figure 1 by boron. A solid solution is studied for the ordered state with the partial occupation of only one sublattice.

of a two-phase mixture in these solid solutions when external tensile stress is applied. The advantages of our CPA calculations lie in the use of the total (and not one-electron) energies, in the inclusion of charge-transfer effects in the CPA, and in our refusal to use the effective pair interactions (see, for example, references [20, 23, 24]). The conclusions on phase stability are based on the total-energy calculations and are more reliable than those based on the sums of one-electron energies. We calculated the Madelung energy properly. It should also be mentioned that the reliability of calculations based on pair interactions is poor. Pair interactions in the case where they are derived from the LMTO CPA (see reference [20], for example) overestimate the tendency towards ordering. Our result on the B2 ordering tendency for the boron atoms on the interstitial sublattice may be obtained in calculations with pair interactions qualitatively but the quantitative accuracy will be lost.

Acknowledgments

This work was supported by the Israel Science Foundation founded by the Israel Academy of Sciences and Humanities (Grant No 380/97-11.7). The author is greatly indebted to D Fuks and V Liubich for their help and discussions during this work. Special acknowledgement is given to A Ruban for his support during the CPA calculations.

References

[1] Krasko G L 1997 *Mater. Sci. Eng.* A **234–236** 1071
[2] Baker I, Li X, Xiao H, Carleton R and George E P 1998 *Intermetallics* **6** 177

[3] Liu C T, Lee E H and McKamey C G 1989 *Scr. Metall.* **23** 875
[4] Franczkiewicz A, Gay A-S and Biscondi M 1998 *Mater. Sci. Eng.* A **258** 108
[5] Chuang T H 1991 *Mater. Sci. Eng.* A **141** 169
[6] Krasko G L 1993–1994 *Int. J. Refract. Hard Met.* **12** 251
[7] Sob M, Wang L G and Vitek V 1997 *Mater. Sci. Eng.* A **234–236** 1075
[8] Ellis D E, Guo J and Low J J 1995 *Electronic Density Functional Theory of Molecules, Clusters, and Solids* ed D E Ellis (Dordrecht: Kluwer) p 263
Jones R O and Gunnarson O 1989 *Rev. Mod. Phys.* **61** 689
[9] Andersen O K 1975 *Phys. Rev.* B **12** 3060
Skriver H L 1984 *The LMTO Method* (New York: Springer)
[10] Ellis D E, Dorfman S, Fuks D, Evenhaim R and Mundim K C 1998 *Int. J. Quantum Chem.* **70** 1085
Berner A, Mundim K C, Ellis D E, Dorfman S, Fuks D and Evenhaim R 1999 *Sensors Actuators* A **74** 86
[11] Eriksson O, Johansson B, Brooks M S S and Skriver H L 1989 *Phys. Rev.* B **40** 9519
[12] Antonov V N, Yavorsky B Yu, Shpak A P, Antonov Vi N, Jepsen O, Guizzetti G and Marabelli F 1996 *Phys. Rev.* B **53** 15 631
[13] Felser C, Kohler J, Simon A and Jepsen O 1998 *Phys. Rev.* B **57** 1510
[14] Blaha P, K, Schwarz, Sorantin P and Trickey S B 1990 *Comput. Phys. Commun.* **59** 399
[15] Christensen A, Ruban A V, Stoltze P, Jacobsen K W, Skriver H L, Norskov J K and Besenbacher F 1997 *Phys. Rev.* B **56** 5822
Landa A I, Ruban A V, Abrikosov I A, Wynblatt P and Skriver H L 1997 *Structure and Evolution of Surfaces (MRS Symposium Proceedings vol 440)* ed R C Cammarata, E H Chason, T L Einstein and S D Williams (Warrendale, PA: Materials Research Society) p 467
[16] Connolly J W D and Williams A R 1983 *Phys. Rev.* B **27** 5169
[17] Faulkner J S 1982 *Prog. Mater. Sci.* **27** 1
[18] Ruban A V, Abrikosov I A and Skriver H L 1995 *Phys. Rev.* B **51** 12 958
[19] Abrikosov I A and Johansson B 1998 *Phys. Rev.* B **57** 14 164
[20] Kudrnovsky J, Turek I and Drchal V 1992 *Lectures on Methods of Electronic Structure Calculations* ed V Kumar, O K Andersen and A Mookerjee (Singapore: World Scientific) and references therein
[21] Krivoglaz M A and Smirnov A A 1964 *The Theory of Order–Disorder in Alloys* (London: Macdonald)
[22] Moruzzi V L, Janak J F and Schwarz K 1988 *Phys. Rev.* B **37** 790
[23] Fuks D and Dorfman S 1995 *J. Physique Coll.* IV **5** C2 135
[24] Dorfman S and Fuks D 1995 *Z. Phys.* B **97** 559